RESEARCH

Biomechanical changes of oblique lumbar interbody fusion with different fixation techniques in degenerative spondylolisthesis lumbar spine: a finite element analysis

Er-Xu Tao[1,2,3], Ren-Jie Zhang[1,2,3], Bo Zhang[1,2,3], Jia-Qi Wang[1,2,3], Lu-Ping Zhou[1,2,3] and Cai-Liang Shen[1,2,3*]

Abstract

Objective   There is a dearth of comprehensive research on the stability of the spinal biomechanical structure when combining Oblique Lumbar Interbody Fusion (OLIF) with internal fixation methods. Hence, we have devised this experiment to meticulously examine and analyze the biomechanical changes that arise from combining OLIF surgery with different internal fixation techniques in patients diagnosed with degenerative lumbar spondylolisthesis.

Methods   Seven validated finite element models were reconstructed based on computed tomography scan images of the L3-L5 segment. These models included the intact model, a stand-alone (S-A) OLIF model, a lateral screw rod (LSR) OLIF model, a bilateral pedicle screw (BPS) OLIF model, an unilateral pedicle screw (UPS) OLIF model, a bilateral CBT (BCBT) OLIF model, and an unilateral CBT(UCBT) OLIF model. The range of motion (ROM), as well as stress levels in the cage, L4 lower endplate, L5 upper endplate, and fixation constructs were assessed across these different model configurations.

Results   S-A model had the highest average ROM of six motion modes, followed by LSR, UPS, UCBT, BPS and BCBT. The BCBT model had a relatively lower cage stress than the others. The maximum peak von Mises stress of the fixation constructs was found in the LSR model. The maximum peak von Mises stress of L4 lower endplate was found in the S-A model. The peak von Mises stress on the L4 lower endplate of the rest surgical models showed no significant difference. The maximum peak von Mises stress of the L5 upper endplate was found in the S-A model. The minimum peak von Mises stress of the L5 upper endplate was found in the BCBT model. No significant difference was found for the peak von Mises stress of the L5 upper endplate among LSR, BPS, UPS and UCBT models.

Conclusion   Among the six different fixation techniques, BCBT exhibited superior biomechanical stability and minimal stress on the cage-endplate interface. It was followed by BPS, UCBT, UPS, and LSR in terms of effectiveness. Conversely, S-A OLIF demonstrated the least stability and resulted in increased stress on both the cage and endplates. Combining OLIF with BCBT fixation technique enhanced biomechanical stability compared to BPS and presented as a less invasive alternative treatment for patients with degenerative lumbar spondylolisthesis.

*Correspondence:
Cai-Liang Shen
shencailiang@ahmu.edu.cn

Full list of author information is available at the end of the article

Introduction

The incidence of lumbar spondylolisthesis is increasing as a result of the growing phenomenon of population aging and the heightened intensity of social labor, thus aligning with the prevailing trend observed in nature. Lumbar spondylolisthesis can be categorized into several types, namely traumatic, pathological, iatrogenic, isthmic, and degenerative spondylolisthesis. Among these classifications, degenerative lumbar spondylolisthesis (DLS) is the most commonly encountered form [1]. Degenerative lumbar spondylolisthesis exhibits a higher prevalence among individuals aged 40 and above, particularly in the L4-L5 segment, with an incidence rate ranging from approximately 5–7% [2]. Furthermore, there is an elevated proportion of women affected by this condition [3]. This condition often leads to lumbar instability and may manifest symptoms such as back pain, lower limb numbness, or intermittent claudication [4]. Conservative management demonstrates limited efficacy in the majority of symptomatic lumbar spondylolisthesis patients, resulting in a significant deterioration of their overall quality of life [5]. For the surgical management of lumbar spondylolisthesis, the predominant approaches have traditionally involved direct decompression and restorative fixation techniques, including posterior lumbar interbody fusion (PLIF) and transforaminal lumbar interbody fusion (TLIF) [6]. With the advancements in channel and endoscopic techniques, minimally invasive surgery TLIF (MIS-TLIF) and endoscope-assisted TLIF (ENDO-TLIF) have emerged as viable options for managing mild (I° and II°) degenerative lumbar spondylolisthesis [7, 8]. While the effectiveness of these techniques has been established in previous literature, it is crucial to acknowledge that they may still lead to significant impairment of the posterior muscle and bone structures [9, 10].

The minimally invasive retroperitoneal anterior approach to the lumbar spine was initially described by Mayer et al. [11]. Subsequently, Silvestre et al. [12]. adopted Mayer's technique for lumbar interbody fusion, which became known as oblique lumbar interbody fusion (OLIF). Initially, this technique was utilized for the management of mild to moderate lumbar spinal stenosis and subsequently expanded to encompass lumbar spondylolisthesis [13]. Furthermore, the OLIF technique aligns with the fundamental principle of reducing lumbar spondylolisthesis by aiming to restore the height of the intervertebral space prior to reduction. Numerous clinical practices have also provided substantial evidence supporting the remarkable efficacy of OLIF in terms of achieving indirect decompression and successful reduction outcomes [14–16]. Cheng et al. [14]. analyzed 79 patients treated with OLIF procedure (61% of the them underwent stand-alone surgery, 19% patients underwent supplemental percutaneous pedicle screw fixation and 20% patients underwent lateral vertebral instrumentation), and they found that the Visual Analogue Scale (VAS) score and the Oswestry Disability Index (ODI) score had significantly decreased at the final follow-up compared to pre-operation in all three groups and the disc height (DH), segmental lumbar lordotic angle (SLL), lumbar lordotic angle (LL), cross-section area (CSA), pelvic tilt (PT), and pelvic incidence-lumbar lordosis (PI-LL) mismatch had also improved by final follow-up. Hung et al. [15]. analyzed 21 patients that underwent OLIF and 41 patients that received MIS-TLIF, and they found that OLIF showed significantly less blood loss and shorter surgery time compared to MIS-TLIF ($p<0.05$) and the improvement in segmental lordosis, coronal balance, ODI and VAS for back pain improvement at post-operative 6 months was significantly more in OLIF group than
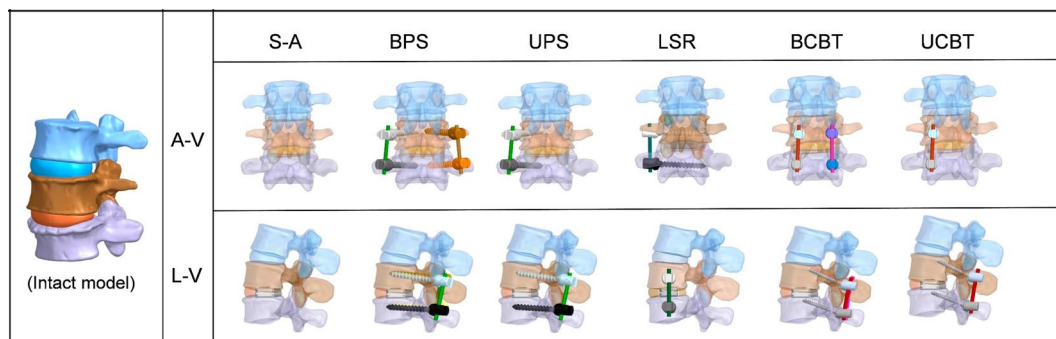

Fig. 1 Each model of the surgical group after assembly. (All cages were placed in the centre of the intervertebral discs) (A-V: Anterior View, L-V: Lateral View, S-A: Stand-Alone, BPS: Bilateral Pedicle Screw, UPS: Unilateral Pedicle Screw, LSR: Lateral Screw Rod, BCBT: Bilateral Cortical Bone Trajectory, UCBT: Unilateral Cortical Bone Trajectory)
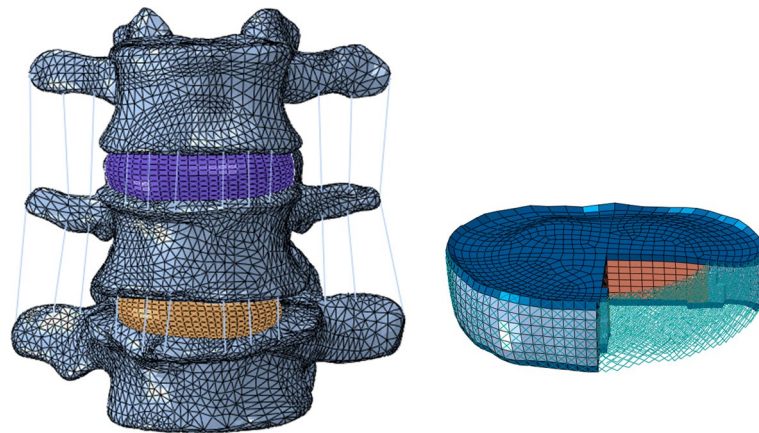
Fig. 2 The intact model and intervertebral disc model

MIS-TLIF group ($p < 0.05$). Shimizu et al. [16]. analyzed 51 patients who underwent OLIF and 41 patients who underwent conventional TLIF and/or PLIF and found that the JOA score improved in both groups at the 1-year follow up (76.6% vs. 73.5% improvement rate in the OLIF and TPLIF groups, respectively) and the fusion rate at the 1-year follow-up was higher in the OLIF group than in the TPLIF group (87.2% vs. 57.4%).

However, the presence of unstable intervertebral relationships in the majority of degenerative lumbar spondylolisthesis cases has sparked ongoing debates regarding the efficacy of OLIF alone in achieving effective stabilization. Notably, several studies conducted by scholars have demonstrated that stand-alone (S-A) OLIF can successfully achieve satisfactory decompression, reduction, and stabilization outcomes [17, 18]. Furthermore, certain scholarly investigations suggest that additional internal fixation may be necessary for degenerative lumbar spondylolisthesis following OLIF [19]. In the context of

Fig. 3 Mesh convergence study

degenerative lumbar spondylolisthesis, there remains a lack of consensus regarding the optimal internal fixation method that can effectively address unstable segments and provide favorable short and long-term fixation outcomes. In light of this, we employed finite element analysis in our study to assess the biomechanical alterations resulting from the combination of OLIF with six different internal fixation methods for degenerative spondylolisthesis in the lumbar spine. This approach offers several advantages over cadaveric studies as it allows for convenient simulation of various internal fixations and facilitates evaluation of complex biomechanical properties.

Materials and methods

In this study, seven finite element models (FEMs) were established based on a degenerative spondylolisthesis lumbar spine. These included the intact lumbar spine, a stand-alone (S-A) OLIF model without instrumentation, a lateral screw-rod (LSR) OLIF model, a bilateral pedicle screw (BPS) OLIF model, a unilateral pedicle screw (UPS) OLIF model, a bilateral cortical bone trajectory (BCBT) OLIF model, and a unilateral cortical bone trajectory (UCBT) OLIF model (Fig. 1). Bilateral pedicle screw fixation is widely recognized as the gold standard in spinal surgery. In this study, we employed bilateral pedicle screw fixation as the reference standard and conducted a comparative analysis of the biomechanical characteristics among five alternative surgical procedures.

Establishment of L3–L5 lumbar spine finite element model

The Radiology Department of the first affiliated hospital of Anhui Medical University provided the data for a 62 years old female patient (L4 degenerative lumbar spondylolisthesis), whose preoperative computerized tomography (CT) scan was 0.625 mm thick per slice. The images of the CT scan were imported into the study MIMICS 15.0 for three-dimensional reconstruction (Materialize, Leuven, Belgium). The data were assembled (Pro/
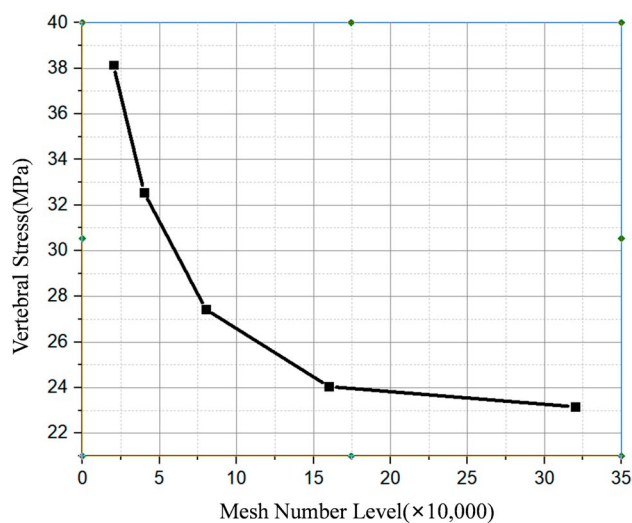
Table 1 Material properties of implant components

	Elastic modulus (MPa)	Poisson's ratio v	Cross-sectional Area (mm²)
Cortical bone of vertebral body	12,000	0.3	/
Cancellous bone of vertebral body	100	0.2	/
Pedicle	3500	0.25	/
Facet joints	15	0.45	/
Endplate	24	0.25	/
Nuclear pulposus	1	0.499	/
Annulus fibrosus	4.2	0.45	/
Anterior longitudinal ligament	7.8	/	63.7
Posterior longitudinal ligament	1	/	20
Ligamentum flavum	1.5	/	40
Capsular ligaments	7.5	/	30
Intertransverse ligaments	10	/	1.8
Interspinous ligaments	1	/	40
Supraspinous ligaments	3	/	30
Spinal instrumentation (titanium alloy)	110,000	0.3	/

E5.0; PTC, MA, USA) into the 3D Finite element model (FEM) of the L3-L5 vertebrae, after restoring, deriving, and spheroidizing (Geomagic Studio15.0; Geomagic, SC, USA). In SolidWorks 2017CAD, the smooth model was imported (SolidWorks Corporation, Concord, MA, USA). The L3-L5 vertebral bodies, posterior elements (including cortical and cancellous bone), intervertebral disks, endplates, and ligamentous system (anterior longitudinal ligament, posterior longitudinal ligament, capsular ligament, intertransverse ligament, ligamentum flavam, interspinous and supraspinous ligament) were all included in the FEM model. The nucleus pulposus (NP) makes up 44% of the intervertebral disk, while the annulus fibrosus (AF) makes up 56% [20]. The collagen fibers of the AF matrix were oriented 30° to 45° to the horizontal plane and ranged from the AF's inner to outer lamina. The elastic behavior of the AF was modeled using the hyperelastic Mooney-Rivlin formulation of eight annulus fiber layers, while the nonlinear structural behavior of the spinal ligaments was modeled using the Maxwell–Kelvin–Voigt visco-elastic law [21]. Annular fibers and ligaments were designed as truss components that could only withstand tensile loads. A surface contact factor was used to model the facet joint, and the coefficient of friction was set to 0.1 [22]. The L4-L5 oblique interbody fusion model was simulated using LSR, traditional trajectory screw (TT) or CBT, interbody fusion cages (36 mm * 16 mm * 10 mm), and grafts placed inside the cage. The TT screw (6.5 mm * 45 mm) was inserted into the vertebral body along the anatomic axis of the pedicle and parallel to the vertebral endplate, while the entry point of the CBT screw (4.5 mm * 30 mm) was determined by drilling at the intersection of line 1 mm inferior to the caudal aspect of the transverse process and a line through the midline of the superior facet, which was approximately 3 mm medial to the lateral margin of pars interarticularis [23–25]. The properties of the materials used in the models were gathered from previous studies [20, 26–28] (Table 1). In order to enhance the accuracy of calculation, the type of mesh in the models are controlled: the mesh type of vertebrae is set as tetrahedral mesh, the mesh type of intervertebral disc is set as hexahedral mesh. There are 218,461 elements and 391,145 nodes in all (Fig. 2). For the model mesh, 20,000, 40,000, 80,000, 160,000 and 320,000 mesh levels were used to encrypt and analyze the vertebrae stress. The results show that the variation error of the result is less than 5% after the number of 320,000 mesh levels is reached. Taking into account the computational efficiency, the whole mesh level is 200,000 to 400,000 (Fig. 3).

Boundary and loading conditions

With fixation on the inferior surface of L5, a vertical axial preload of 150 N was applied to the superior surface of the L3 vertebral bodies, while bending moments of 10 N/m were exerted on the L3 superior surface to simulate six different physiological motions: flexion, extension, left lateral bending, right lateral bending, left rotation, and right rotation (Fig. 4).

Measurement data

The Range of Motion (ROM), the peak von Mises stress of the cage, the stress of the endplate, and the stress of internal fixation under different loading conditions were compared to investigate the biomechanical stability of various instruments.
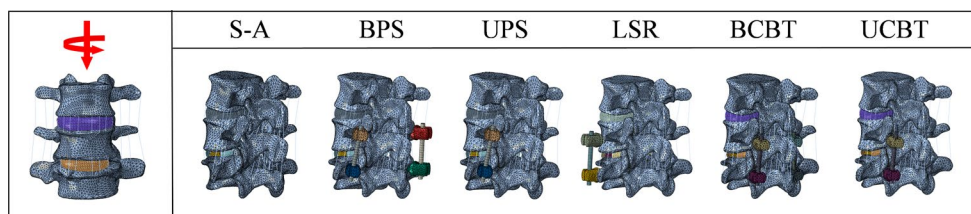

Fig. 4 Boundary and loading conditions of finite element models

Model validation

By comparing the ROM data of the intact model consisting of L3-L4, L4-L5 to previous experimental data obtained from cadaveric and finite element studies, the ROM data of the intact model consisting of L3-L4, L4-L5 were confirmed.

Results

Validation of the intact model

We compared our ROM data of the intact model to previous cadaveric and FE studies under the similar loads to our model [29, 30]. The average ROM of the intact model established by us under the six motion modes in the L3-4 segment was 4.123°, which is 17.8% higher than the model established by Yamamoto et al., and 2.43% higher than the model established by Huang et al. The average ROM of the six motion modes in our intact model at L4-5 segment was 4.183°, which increased by 9.13% compared with the model established by Yamamoto et al., while decreased by 8.43% compared with the model established by Huang et al. Therefore, Our results were in good agreement with previously reported data (Fig. 5).

Range of motion

The ROM of all surgical models was lower than that of the intact model. The ROM of S-A model was higher than that of the BPS model in all motion modes (increased by 26.63%, 44.99%, 21.70%, 2.48%, 22.34%, 10.99%, in flexion, extension, left lateral bending, right lateral bending, left rotation, right rotation, respectively). The LSR model had a higher ROM than the BPS model in extension, left lateral bending, and right rotation motion modes (increased by 13.77%, 30.94%, 0.08%, respectively), but a lower ROM in flexion, right lateral bending and left rotation motion modes (decreased by 6.13%, 0.09%, 0.09%, respectively). The UPS model had a higher ROM than the BPS model in all motion modes (increased by 20.51%, 21.74%, 20.66%, 1.24%, 40.87%, 18.93%, in flexion, extension, left lateral bending, right lateral bending, left rotation and right rotation, respectively). Compared with BPS model, the ROM of UCBT model was

lower (decreased by 15.53%, 4.00%, 17.88% in right lateral bending, left rotation and right rotation, respectively), except that the ROM of UCBT model was higher in flexion, extension and left lateral bending motion modes (increased by 14.38%, 11.27%, 8.72%, respectively). In contrast to the BPS model, the ROM of BCBT model was lower in all motion modes (decreased by 22.77%, 16.46%, 19.52%, 34.16%, 7.27%, 10.59%, in flexion, extension, left lateral bending, right lateral bending, left rotation and right rotation, respectively). The ROM of the surgical and intact models is shown in Fig. 6.

Stress of the cage

There was no significant difference in the peak von Mises stress of the cage to be found among S-A, LSR, UPS, BPS and UCBT models. While the BCBT model had a relatively lower cage stress than the others. Figures 7 and 8 shows the peak von Mises stress of the cage for different models in six motion modes.

Stress of the fixation constructs

The maximum peak von Mises stress of the fixation constructs was found in the LSR model (Figs. 9 and 10). During left lateral bending and right lateral bending motion modes, the stress experienced by the screws in the LSR model was 224.15% and 123.80% higher than that in the BPS model.

Stress of L4 lower endplate

The peak von Mises stress on the L4 lower endplate of all surgical models was higher than that of the intact model. The maximum peak von Mises stress of L4 lower endplate was found in the S-A model. The peak von Mises stress on the L4 lower endplate of the rest surgical models showed no significant difference. Figures 11 and 12 shows the peak von Mises stress of the L4 lower endplate for different models in six motion modes.

Stress of L5 upper endplate

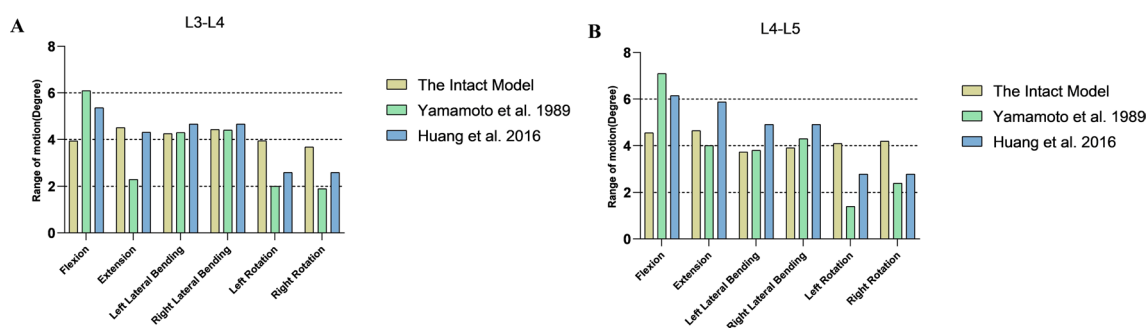The peak von Mises stress on the L5 upper endplate of all surgical models was higher than that of the intact model.

Fig. 5 ROM comparisons between the intact model and previously published studies at the L3-L4 (**A**) and L4-L5 (**B**) levels
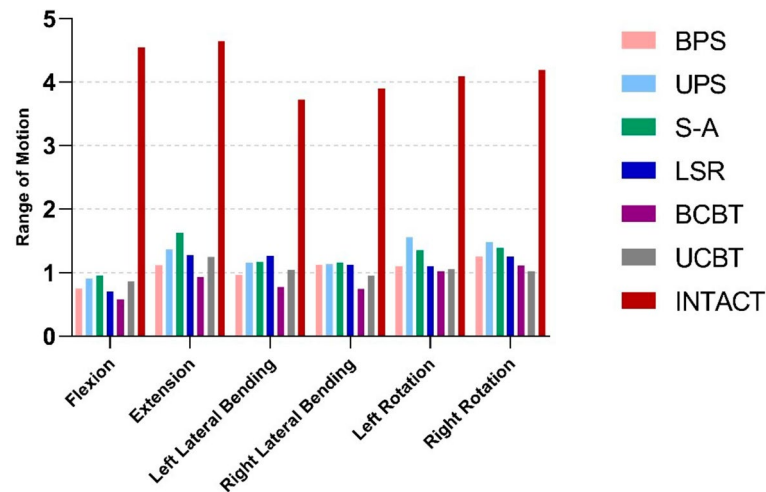
Fig. 6 The ROM of surgical and intact models under different motion modes. (S-A: stand-alone, BPS: bilateral pedicle screw, UPS: unilateral pedicle screw, LSR: lateral screw rod, BCBT: bilateral cortical bone trajectory screw, UCBT: unilateral cortical bone trajectory screw)

Fig. 7 The peak von Mises stress on cage of surgical models under different motion modes. (S-A: stand-alone, BPS: bilateral pedicle screw, UPS: unilateral pedicle screw, LSR: lateral screw rod, BCBT: bilateral cortical bone trajectory screw, UCBT: unilateral cortical bone trajectory screw)
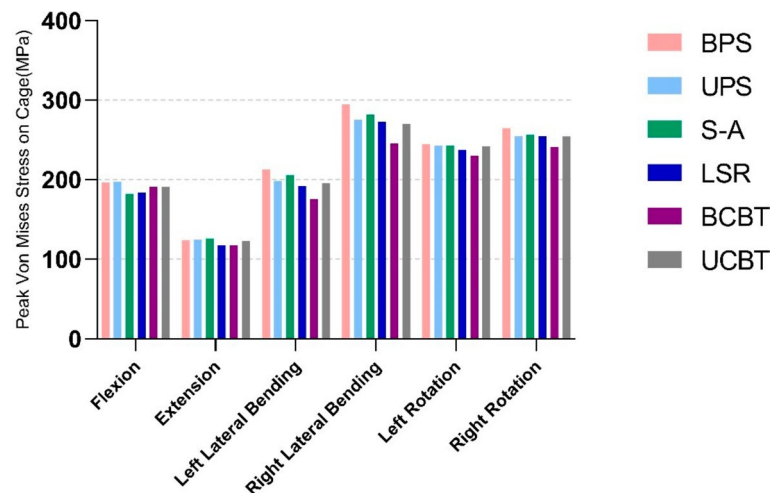
The maximum peak von Mises stress of the L5 upper endplate was found in the S-A model. The minimum peak von Mises stress of the L5 upper endplate was found in the BCBT model. No significant difference was found for the peak von Mises stress of the L5 upper endplate among LSR, BPS, UPS and UCBT models. Figures 13 and 14 shows the peak von Mises stress of the L5 upper endplate for different models in six motion modes.

Discussion

Lumbar fusion is a clinically effective treatment for degenerative lumbar spondylolisthesis. Currently, commonly utilized surgical techniques such as posterior lumbar interbody fusion (PLIF) and transforaminal lumbar interbody fusion (TLIF) exhibit definite clinical efficacy; however, they unavoidably entail drawbacks including significant blood loss, prolonged hospitalization, and

potential damage to the stability structure of the posterior column of the spine [31–34]. Compared to PLIF and TLIF techniques, OLIF offers a distinct advantage by accessing the target disc through the anatomical window between the abdominal major vessels and the psoas muscle [7]. Consequently, this approach significantly reduces the risk of lumbar plexus injury and minimizes extensive dissection of paraspinal muscles [35]. The favorable outcomes observed following an OLIF procedure can be attributed to various factors including restoration of disc height, enlargement of foraminal area, correction of coronal balance, as well as indirect decompression of neural elements facilitated by larger implants [36, 37]. Although the novel surgical approach offers numerous advantages, it is crucial to acknowledge that fusion of the surgical segment still occurs through the insertion of an allografted cage. Consequently, there has been a growing
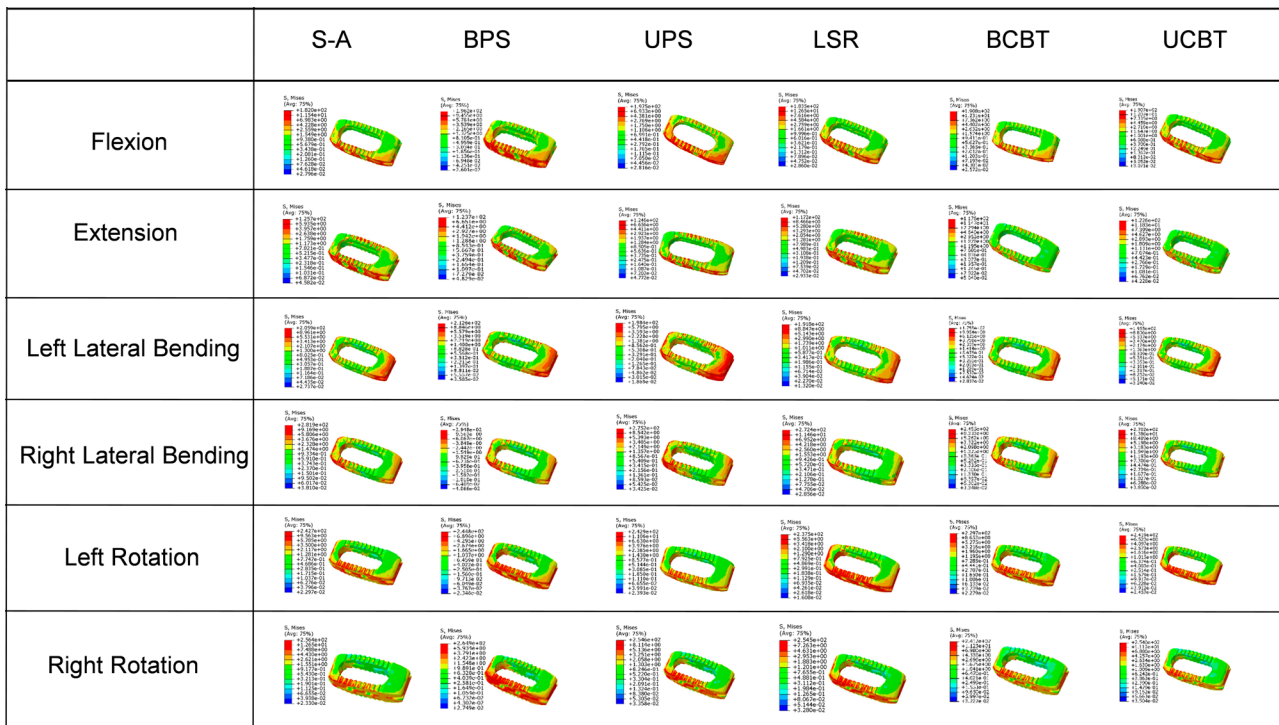
	S-A	BPS	UPS	LSR	BCBT	UCBT
Flexion						
Extension						
Left Lateral Bending						
Right Lateral Bending						
Left Rotation						
Right Rotation						

Fig. 8 Von Mises stress distribution on the OLIF cages, with different fixation techniques in degenerative spondylolisthesis lumbar spine under different motion modes. (S-A: stand-alone, BPS: bilateral pedicle screw, UPS: unilateral pedicle screw, LSR: lateral screw rod, BCBT: bilateral cortical bone trajectory screw, UCBT: unilateral cortical bone trajectory screw)

Fig. 9 The peak von Mises stress on fixation constructs of surgical models under different motion modes. (BPS: bilateral pedicle screw, UPS: unilateral pedicle screw, LSR: lateral screw rod, BCBT: bilateral cortical bone trajectory screw, UCBT: unilateral cortical bone trajectory screw)
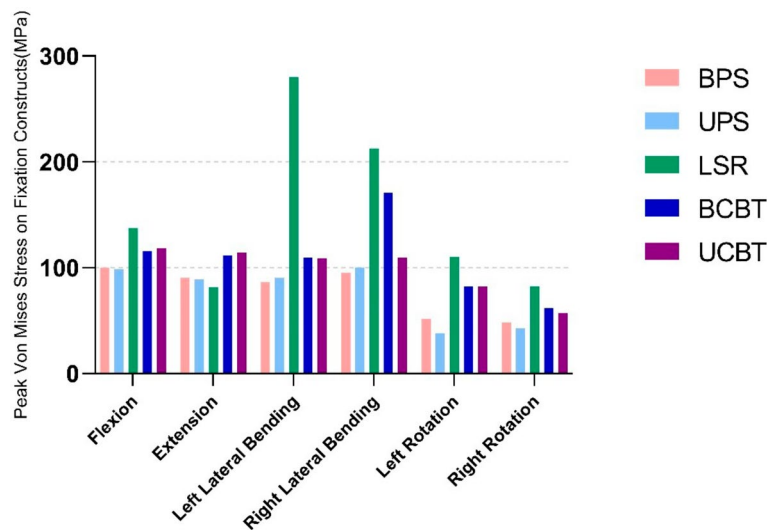
emphasis on mitigating cage subsidence in OLIF and ensuring optimal postoperative outcomes for patients.

The occurrence of subsidence is contingent upon various factors, such as compromised bone quality in patients, endplate injury during surgical procedures, excessive distraction, utilization of small cages for fusion, and different types of internal fixation constructs [38, 39]. Among the aforementioned factors, diverse forms of internal fixation constructs play a pivotal role in upholding surgical segment stability and mitigating cage subsidence [40]. Previous studies using finite element analysis have assessed the biomechanical alterations of OLIF combined with various fixation techniques in a normal lumbar spine, including stand-alone OLIF [41],
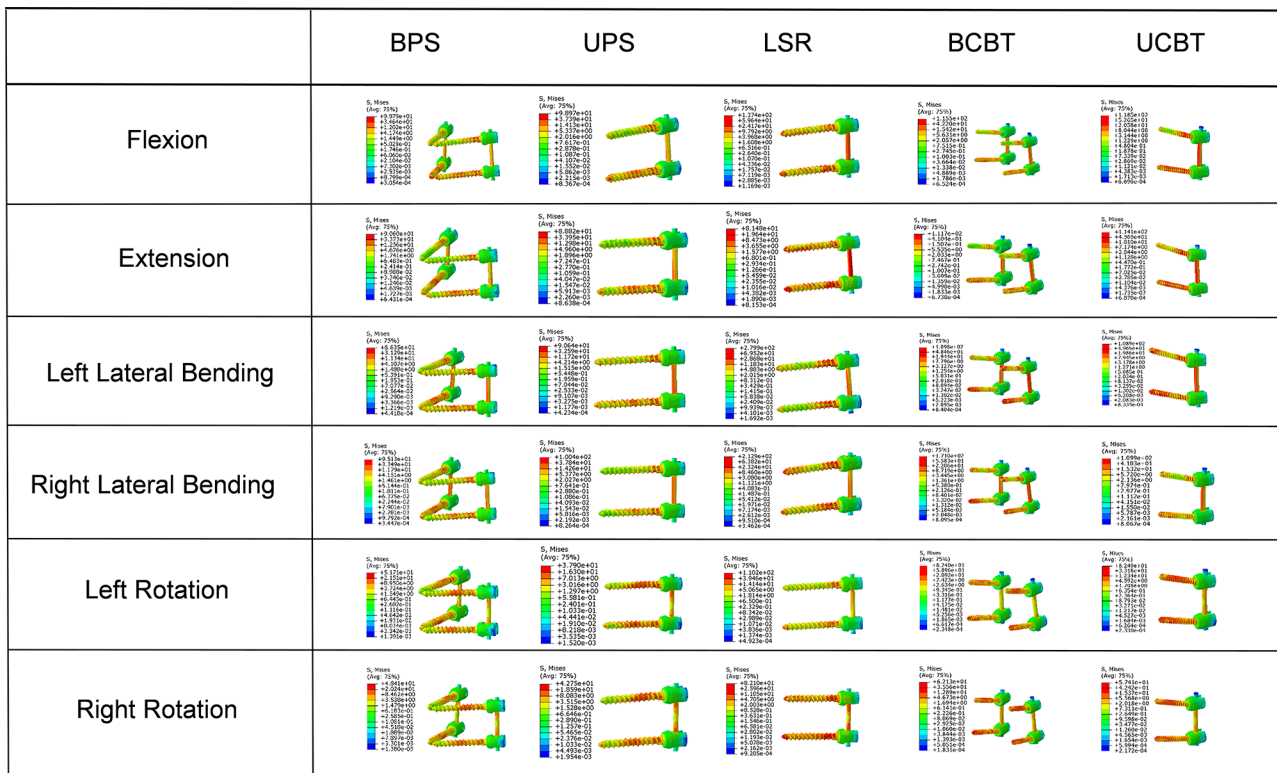
Fig. 10 Von Mises stress distribution on the fixation constructs, with different fixation techniques in degenerative spondylolisthesis lumbar spine under different motion modes. (S-A: stand-alone, BPS: bilateral pedicle screw, UPS: unilateral pedicle screw, LSR: lateral screw rod, BCBT: bilateral cortical bone trajectory screw, UCBT: unilateral cortical bone trajectory screw)

Fig. 11 The peak von Mises stress on L4 lower endplate of surgical and intact models under different motion modes. (S-A: stand-alone, BPS: bilateral pedicle screw, UPS: unilateral pedicle screw, LSR: lateral screw rod, BCBT: bilateral cortical bone trajectory screw, UCBT: unilateral cortical bone trajectory screw)
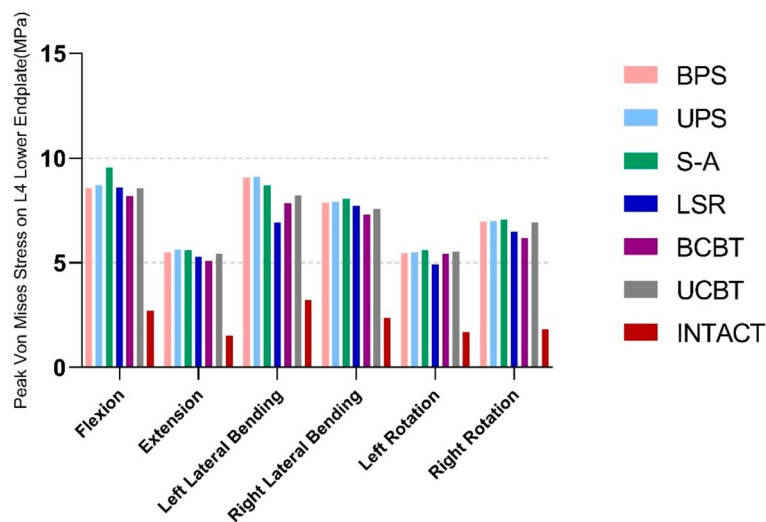
lateral rod-screw fixation [42], posterior pedicle screw fixation [43], and translaminar facet screw fixation [31, 44]. However, there is a dearth of research investigating the biomechanical changes of OLIF with different fixation techniques specifically in degenerative spondylolisthesis of the lumbar spine.

In contrast to the instrumented models, the S-A model exhibited the greatest range of motion (ROM), highest stress on the lower endplate of L4, upper endplate of L5, and cage stress. These findings suggest a potential risk factor for cage subsidence. Previous finite element studies have also demonstrated that OLIF surgery using the
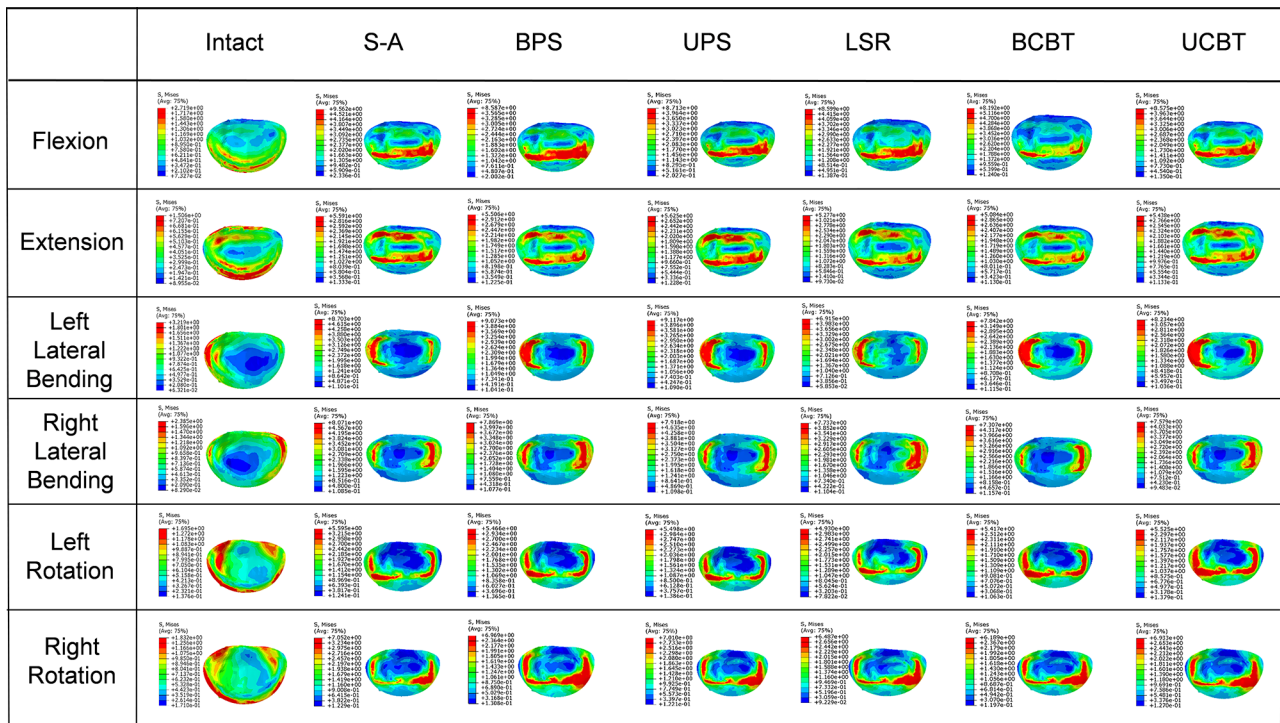
Fig. 12 Von Mises stress distribution on the lower endplates of the L4 vertebra, with different fixation techniques in degenerative spondylolisthesis lumbar spine under different motion modes. (S-A: stand-alone, BPS: bilateral pedicle screw, UPS: unilateral pedicle screw, LSR: lateral screw rod, BCBT: bilateral cortical bone trajectory screw, UCBT: unilateral cortical bone trajectory screw)

Fig. 13 The peak von Mises stress on L5 upper endplate of surgical and intact models under different motion modes. (S-A: stand-alone, BPS: bilateral pedicle screw, UPS: unilateral pedicle screw, LSR: lateral screw rod, BCBT: bilateral cortical bone trajectory screw, UCBT: unilateral cortical bone trajectory screw)
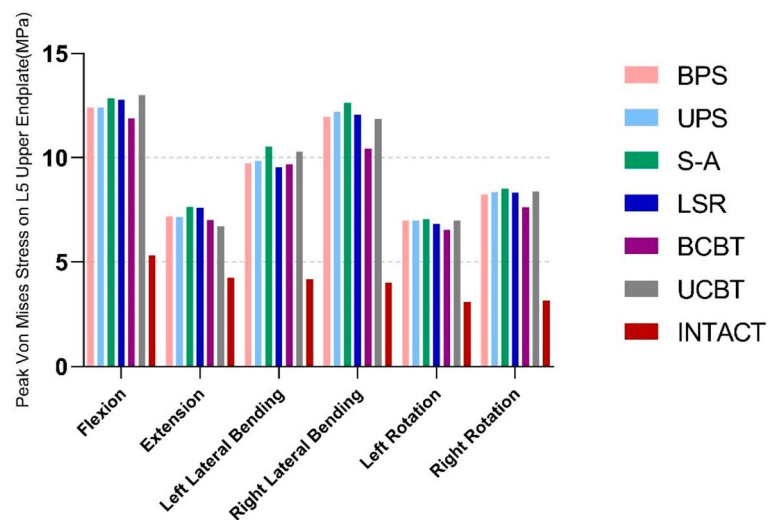
S-A method resulted in increased ROM and greater cage stress compared to OLIF with BPS, particularly during extension and flexion motions [19]. Thus, S-A OLIF does not guarantee solid fixation, and supplementary fixation constructs, such as lateral screw-rods or pedicle screws, are necessary to distribute the load across the vertebra and prevent cage subsidence.

Bilateral pedicle screw fixation has been extensively employed as a posterior fixation construct following OLIF and is considered the benchmark for managing degenerative and traumatic spinal diseases due to its rigid structural characteristics [31]. In this study, BPS exhibited biomechanical properties that were deemed acceptable, aligning with previous research findings
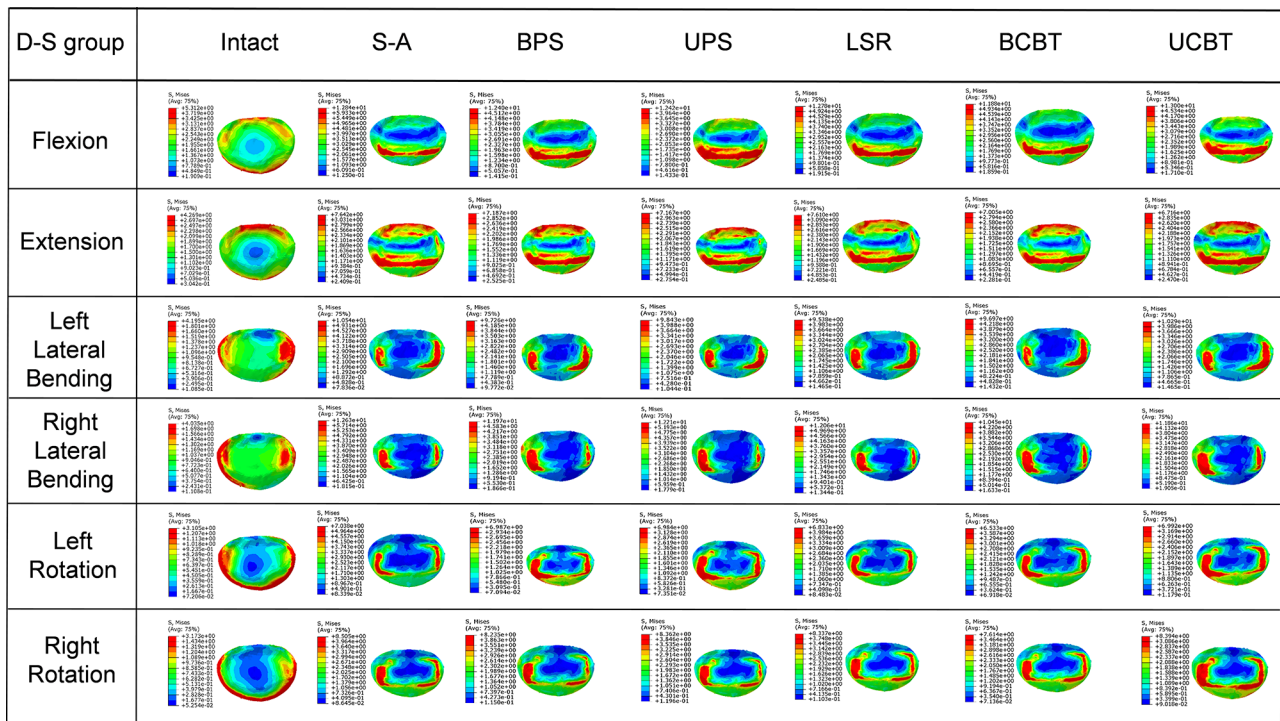
Fig. 14 Von Mises stress distribution on the upper endplates of the L5 vertebra, with different fixation techniques in degenerative spondylolisthesis lumbar spine under different motion modes. (S-A: stand-alone, BPS: bilateral pedicle screw, UPS: unilateral pedicle screw, LSR: lateral screw rod, BCBT: bilateral cortical bone trajectory screw, UCBT: unilateral cortical bone trajectory screw)

[31, 45–47]. Nevertheless, the BPS fixation method still presents certain limitations including substantial blood loss, extensive dissection of paravertebral muscles, facet joint violation, neurological risks, vascular injuries, and increased surgical duration. Although UPS exhibits slightly lower biomechanical stability compared to BPS, it effectively mitigates damage to paraspinal muscles and perioperative bleeding while also reducing instrument expenses. Consequently, UPS emerges as a promising alternative to BPS internal fixation technology, offering potential advancements in the field of spinal surgery.

Compared to BPS, LSR exhibited a slight decrease in cage stress compared to the BPS model. In addition, the histogram of peak von Mises stress in the LSR model and the corresponding stress distribution thermal map reveal that the internal fixation device experiences higher peak stress compared to the BPS model. Moreover, this stress is predominantly concentrated at the junction between the screw and cortical bone, thereby substantially increasing the risk of postoperative screw breakage. Therefore, considering the biomechanical characteristics of the operative segment, LSR may be suitable for carefully selected patients with good bone quality and normal body mass index.

CBT screw fixation has been developed and clinically utilized in osteoporotic patients by Santoni et al. since 2009 [48]. Matsukawa et al. [49] noted that the bone mineral density of the femoral neck, screw length within the lamina, and cephalad angle were significant independent factors influencing torque and CBT screw fixation, which varied based on technical factors (cephalad angle and screw length within the lamina) as well as individual patient characteristics such as bone mineral density. The optimal trajectory was determined to be directed cranially at an angle of 25° to 30° along the inferior border of the pedicle to achieve maximum contact with the lamina and sufficient length within the vertebral body. Our study findings indicate that the BCBT screw fixation technique offers enhanced spinal stability and decreased stress on both the cage and endplate when compared with BPS fixation for degenerative spondylolisthesis in the lumbar spine. Additionally, we observed similar biomechanical properties between UCBT screw fixation technique and BPS fixation for degenerative lumbar spondylolisthesis. Interestingly, despite the higher Peak von Mises stress observed in the internal fixation device of both the BCBT model and UCBT model compared to the BPS model, it is noteworthy that the stress distribution thermal map in these models exhibits a more uniform pattern. This can be attributed to an adequate contact between screws and cortical bone. Consequently, we assume that the probability of postoperative screw breakage in both the BCBT model and UCBT model would be relatively low. Thus, considering its advantageous biomechanical features,

employing CBT screw fixation method could be a valuable substitute for BPS fixation during OLIF procedures targeting degenerative spondylolisthesis in the lumbar spine.

There are several limitations in this study. Firstly, as a computer simulated biomechanical experiment, it inherently possesses certain inherent disadvantages. The simulated material properties are oversimplified and idealized. Future analyses should consider incorporating more accurate geometry and material properties into the simulation. Secondly, the study did not observe the biomechanical properties of adjacent segments after OLIF, thus hindering an assessment of the risk of adjacent segment disease. Thirdly, CBT screw fixation is predominantly utilized in patients with osteoporosis; however, this finite element analysis was conducted on patients with normal bone density and therefore cannot fully reflect the biomechanical changes occurring at the fixed segment under conditions of osteopenia. Additionally, the occurrence of complications such as adjacent segment disease, cage subsidence, and endplate fracture is influenced not only by the range of motion of the fixed segment and the stress on the endplate and cage but also by factors such as intraoperative cage model selection, cage placement selection, and patient's body mass index. Furthermore, this study exclusively examined L4 spondylolisthesis, thus limiting the generalizability of its findings to other segments where degenerative lumbar spondylolisthesis may occur. Consequently, further investigations should focus on elucidating the biomechanical alterations associated with spondylolisthesis in these alternative segments. Finally, it is worth noting that our biomechanical study solely focused on single-level fixation; therefore, future research should consider investigating the biomechanical changes associated with these fixation techniques at multiple levels.

Conclusion

Among the six different fixation techniques, BCBT exhibited superior biomechanical stability and minimal stress on the cage-endplate interface. It was followed by BPS, UCBT, UPS, and LSR in terms of effectiveness. Conversely, S-A OLIF demonstrated the least stability and resulted in increased stress on both the cage and endplates. Combining OLIF with BCBT fixation technique enhanced biomechanical stability compared to BPS and presented as a less invasive alternative treatment for patients with degenerative lumbar spondylolisthesis.

Abbreviations

OLIF	Oblique Lumbar Interbody Fusion
PLIF	Posterior Lumbar Interbody Fusion
TLIF	Transforaminal Lumbar Interbody Fusion
MIS-TLIF	Minimally Invasive Surgery TLIF
ENDO-TLIF	Endoscope-Assisted TLIF
DLS	Degenerative Lumbar Spondylolisthesis
FEMs	Finite Element Models
S-A	Stand Alone
BPS	Bilateral Pedicle Screw
UPS	Unilateral Pedicle Screw
LSR	Lateral Screw Rod
BCBT	Bilateral Cortical Bone Trajectory
UCBT	Unilateral Cortical Bone Trajectory
ROM	Range of Motion
VAS	Visual Analogue Scale
ODI	Oswestry Disability Index

Declarations

Ethics approval and consent to participate
This study was approved by the Ethics Committee of the first affiliated hospital of Anhui Medical University. All subjects signed informed consent by each patient. All clinical investigations had been conducted according to the principles expressed in the Declaration of Helsinki.

Consent for publication
Not applicable.

Competing interests
The authors declare no competing interests.

Author details
[1]Department of Orthopedics and Spine Surgery, The First Affiliated Hospital of Anhui Medical University, 218 Jixi Road, Hefei, Anhui 230022, China
[2]Laboratory of Spinal and Spinal Cord Injury Regeneration and Repair, The First Affiliated Hospital of Anhui Medical University, 218 Jixi Road, Hefei, Anhui 230022, China
[3]Anhui Province Research Center for the Clinical Application of Digital Medical Technology, The First Affiliated Hospital of Anhui Medical University, 218 Jixi Road, Hefei, Anhui 230022, China

References
1. Wang PT, Zhang JN, Liu TJ, Yang JS, Hao DJ. Comparison of degenerative lumbar spondylolisthesis and isthmic lumbar spondylolisthesis: effect of pedicle screw placement on proximal facet invasion in surgical treatment. BMC Musculoskelet Disord. 2022;23(1):6. Published 2022 Jan 3. https://doi.org/10.1186/s12891-021-04962-7
2. 2, Aoki Y, Takahashi H, Nakajima A, et al. Prevalence of lumbar spondylolysis and spondylolisthesis in patients with degenerative spinal disease. Sci Rep. 2020;10(1):6739. Published 2020 Apr 21 https://doi.org/10.1038/s41598-020-63784-0.

3.   Norton RPBK, Klifto C, Errico TJ, Bendo JA. Degenerative spondylolisthesis: an analysis of the Nationwide Inpatient Sample Database. Spine (Phila Pa 1976). 2015;40(15):1219–27.
4.   Chan AKSV, Robinson LC, Mummaneni PV. Summary of guidelines for the treatment of lumbar spondylolisthesis. Neurosurg Clin N Am. 2019;30(3):353–64.
5.   Bydon MAM, Goyal A. Degenerative lumbar spondylolisthesis: definition, natural history, Conservative Management, and Surgical Treatment. Neurosurg Clin N Am. 2019;30(3):299–304. https://doi.org/10.1016/j.nec.2019.02.003.
6.   de Kunder SL, van Kuijk SMJ, Rijkers K, et al. Transforaminal lumbar interbody fusion (TLIF) versus posterior lumbar interbody fusion (PLIF) in lumbar spondylolisthesis: a systematic review and meta-analysis. Spine J. 2017;17(11):1712–21. https://doi.org/10.1016/j.spinee.2017.06.018.
7.   Mobbs RJ, Phan K, Malham G, Seex K, Rao PJ. Lumbar interbody fusion: techniques, indications and comparison of interbody fusion options including PLIF, TLIF, MI-TLIF. OLIF/ATP, LLIF and ALIF. J Spine Surg. 2015;1(1):2–18. https://doi.org/10.3978/j.issn.2414-469X.2015.10.05
8.   Kim HSWP, Jang IT. Current and future of endoscopic spine surgery: what are the common procedures we have now and what lies ahead? World Neurosurg. 2020;140:642–53. https://doi.org/10.1016/j.wneu.2020.03.111.
9.   Ahn YYM, Heo DH. Endoscopic transforaminal lumbar interbody fusion: a comprehensive review. Expert Rev Med Devices. 2019;16(5):373–80. https://doi.org/10.1080/17434440.2019.1610388.
10. Ge DHSN, Varlotta CG et al. Comparative analysis of two transforaminal lumbar Interbody Fusion techniques: open TLIF Versus Wiltse MIS TLIF. Spine (Phila Pa 1976). 2019;44(9):E555–60. https://doi.org/10.1097/BRS.0000000000002903
11. Mayer HM. A new microsurgical technique for minimally invasive anterior lumbar interbody fusion. Spine (Phila Pa 1976). 1997;22(6):691–700. https://doi.org/10.1097/00007632-199703150-00023.
12. Silvestre CM-TJ, Hilmi R, Roussouly P. Complications and morbidities of mini-open anterior retroperitoneal lumbar Interbody Fusion: oblique lumbar Interbody Fusion in 179 patients. Asian Spine J. 2012;6(2):89–97. https://doi.org/10.4184/asj.2012.6.2.89.
13. Li RSX, Li X, Liu Y, Jiang W. Comparison of clinical outcomes and spino-pelvic sagittal balance in degenerative lumbar spondylolisthesis: minimally invasive oblique lumbar interbody fusion (OLIF) versus transforaminal lumbar interbody fusion (TLIF). Med (Baltim). 2021;100(3):e23783. https://doi.org/10.1097/MD.0000000000023783.
14. Cheng CWK, Zhang C, Wu H, Jian F. Clinical results and complications associated with oblique lumbar interbody fusion technique. Ann Transl Med. 2021;9(1):16. https://doi.org/10.21037/atm-20-2159.
15. Hung SFLJ, Tsai TT, et al. Comparison of outcomes between indirect decompression of oblique lumbar interbody fusion and MIS-TLIF in one single-level lumbar spondylosis. Sci Rep. 2021;11(1):12783. https://doi.org/10.1038/s41598-021-92330-9. Published 2021 Jun 17.
16. Shimizu TFS, Otsuki B, Murata K, Matsuda S. Indirect decompression via oblique lateral interbody fusion for severe degenerative lumbar spinal stenosis: a comparative study with direct decompression transforaminal/posterior lumbar interbody fusion. Spine J. 2021;21(6):963–71. https://doi.org/10.1016/j.spinee.2021.01.025.
17. Liu JDW, Yang D, et al. Modic changes (MCs) Associated with Endplate Sclerosis can prevent cage subsidence in oblique lumbar Interbody Fusion (OLIF) stand-alone. World Neurosurg. 2020;138:e160–8. https://doi.org/10.1016/j.wneu.2020.02.047.
18. Hu ZHD, Gao J, et al. The influence of Endplate morphology on cage subsidence in patients with stand-alone oblique lateral lumbar Interbody Fusion (OLIF) [published online ahead of print, 2021 Mar 9]. Global Spine J. 2021;2192568221992098. https://doi.org/10.1177/2192568221992098.
19. Fang GLY, Wu J, et al. Biomechanical comparison of stand-alone and bilateral pedicle screw fixation for oblique lumbar Interbody Fusion Surgery-A finite element analysis. World Neurosurg. 2020;141:e204–12. https://doi.org/10.1016/j.wneu.2020.05.245.
20. Liu X, Ma J, Park P, Huang X, Xie N, Ye X. Biomechanical comparison of multi-level lateral interbody fusion with and without supplementary instrumentation: a three-dimensional finite element study. BMC Musculoskelet Disord. 2017;18(1):63. https://doi.org/10.1186/s12891-017-1387-6. Published 2017 Feb 2.
21. Schmidt H, Heuer F, Simon U, et al. Application of a new calibration method for a three-dimensional finite element model of a human lumbar annulus fibrosus. Clin Biomech (Bristol Avon). 2006;21(4):337–44. https://doi.org/10.1016/j.clinbiomech.2005.12.001.
22. Polikeit A, Ferguson SJ, Nolte LP, Orr TE. Factors influencing stresses in the lumbar spine after the insertion of intervertebral cages: finite element analysis. Eur Spine J. 2003;12(4):413–20. https://doi.org/10.1007/s00586-002-0505-8.
23. Li HM, Zhang RJ, Gao H, et al. Biomechanical fixation properties of the cortical bone trajectory in the osteoporotic lumbar spine. World Neurosurg. 2018;119:e717–27. https://doi.org/10.1016/j.wneu.2018.07.253.
24. Zhang RJ, Li HM, Gao H, et al. Cortical bone trajectory screws used to save failed traditional trajectory screws in the osteoporotic lumbar spine and vice versa: a human cadaveric biomechanical study. J Neurosurg Spine Published Online March. 2019;8. https://doi.org/10.3171/2018.12.SPINE18970.
25. Weinstein JN, Spratt KF, Spengler D, Brick C, Reid S. Spinal pedicle fixation: reliability and validity of roentgenogram-based assessment and surgical factors on successful screw placement. Spine (Phila Pa 1976). 1988;13(9):1012–8.
26. Shim CSPS, Lee SH, Lim TJ, Chun K, Kim DH. Biomechanical evaluation of an interspinous stabilizing device, Locker. Spine (Phila Pa 1976). 2008;33(22):E820–7. https://doi.org/10.1097/BRS.0b013e3181894fb1.
27. Guo HZ, Guo DQ, Tang YC, Liang D, Zhang SC. Selective cement augmentation of cranial and caudal pedicle screws provides comparable stability to augmentation on all segments in the osteoporotic spine: a finite element analysis. Ann Transl Med. 2020;8(21):1384. https://doi.org/10.21037/atm-20-2246.
28. Erbulut DU, Zafarparandeh I, Hassan CR, Lazoglu I, Ozer AF. Determination of the biomechanical effect of an interspinous process device on implanted and adjacent lumbar spinal segments using a hybrid testing protocol: a finite-element study. J Neurosurg Spine. 2015;23(2):200–8. https://doi.org/10.3171/2014.12.SPINE14419.
29. Yamamoto IPM, Crisco T, Oxland T. Three-dimensional movements of the whole lumbar spine and lumbosacral joint. Spine (Phila Pa 1976). 1989;14(11):1256–60. https://doi.org/10.1097/00007632-198911000-00020.
30. Huang YPDC, Cheng CK et al. Preserving Posterior Complex Can Prevent Adjacent Segment Disease following Posterior Lumbar Interbody Fusion Surgeries: A Finite Element Analysis [published correction appears in PLoS One. 2017;12 (2):e0172329]. PLoS One. 2016;11(11):e0166452. Published 2016 Nov 21. https://doi.org/10.1371/journal.pone.0166452
31. Guo HZTY, Guo DQ, et al. The cement leakage in cement-augmented pedicle screw instrumentation in degenerative lumbosacral diseases: a retrospective analysis of 202 cases and 950 augmented pedicle screws. Eur Spine J. 2019;28(7):1661–9. https://doi.org/10.1007/s00586-019-05985-4.
32. Teng IHJ, Phan K, Mobbs R. A meta-analysis comparing ALIF, PLIF, TLIF and LLIF. J Clin Neurosci. 2017;44:11–7. https://doi.org/10.1016/j.jocn.2017.06.013.
33. de Kunder SL, vKS, Rijkers K, et al. Transforaminal lumbar interbody fusion (TLIF) versus posterior lumbar interbody fusion (PLIF) in lumbar spondylolisthesis: a systematic review and meta-analysis. Spine J. 2017;17(11):1712–21. https://doi.org/10.1016/j.spinee.2017.06.018.
34. Fleege CRM, Rauschmann M. PLIF- und TLIF-Verfahren. Indikation, Technik, Vor- Und Nachteile [The PLIF and TLIF techniques. Indication, technique, advantages, and disadvantages]. Orthopade. 2015;44(2):114–23. https://doi.org/10.1007/s00132-014-3065-9.
35. Abe K, Orita S, Mannoji C, et al. Perioperative complications in 155 patients who underwent oblique lateral Interbody Fusion surgery: perspectives and indications from a Retrospective, Multicenter Survey. Spine (Phila Pa 1976). 2017;42(1):55–62. https://doi.org/10.1097/BRS.0000000000001650.
36. Woods KRBJ, Hynes RA. Technical description of oblique lateral interbody fusion at L1-L5 (OLIF25) and at L5-S1 (OLIF51) and evaluation of complication and fusion rates. Spine J. 2017;17(4):545–53. https://doi.org/10.1016/j.spinee.2016.10.026.
37. Sardhara JSS, Mehrotra A, et al. Neuro-navigation assisted pre-psoas minimally invasive oblique lumbar interbody fusion (MI-OLIF): new roads and impediments. Neurol India. 2019;67(3):803–12. https://doi.org/10.4103/0028-3886.263262.
38. Cao YLF, Wan S, et al. Biomechanical evaluation of different surgical procedures in single-level transforaminal lumbar interbody fusion in vitro. Clin Biomech (Bristol Avon). 2017;49:91–5. https://doi.org/10.1016/j.clinbiomech.2017.08.011.
39. Quillo-Olvera JLG, Jo HJ, Kim JS. Complications on minimally invasive oblique lumbar interbody fusion at L2-L5 levels: a review of the literature and surgical strategies. Ann Transl Med. 2018;6(6):101. https://doi.org/10.21037/atm.2018.01.22.
40. Xu DSWC, Godzik J, Turner JD, Smith W, Uribe JS. Minimally invasive anterior, lateral, and oblique lumbar interbody fusion: a literature review. Ann Transl Med. 2018;6(6):104. https://doi.org/10.21037/atm.2018.03.24.

41. Zhu GHY, Yu L, Cai Y, Yang X. Comparing stand-alone oblique lumbar interbody fusion with posterior lumbar interbody fusion for revision of rostral adjacent segment disease: a STROBE-compliant study. Med (Baltim). 2018;97(40):e12680. https://doi.org/10.1097/MD.0000000000012680.

42. Chen YL, Zhu ZH, Wang YK, et al. Zhonghua Yi Xue Za Zhi. 2018;98(25):1990–5. https://doi.org/10.3760/cma.j.issn.0376-2491.2018.25.005.

43. Patel RSSS, Kang SH et al. The radiologic and clinical outcomes of oblique lateral Interbody Fusion for correction of adult, 10, degenerative lumbar Deformity[J]. Indian J Orthop, 53(4):502–9.

44. Kim SMLT, Paterno J, Kim DH. A biomechanical comparison of supplementary posterior translaminar facet and transfacetopedicular screw fixation after anterior lumbar interbody fusion. J Neurosurg Spine. 2004;1(1):101–7. https://doi.org/10.3171/spi.2004.1.1.0101.

45. Guo HZ, Tang YC, Guo DQ, Liang D, Zhang SC. Biomechanical evaluation of four different posterior instrumentation techniques for single-level transforaminal lumbar interbody fusion: a finite element analysis. Am J Translational Res. 2020;12(10):6160–9.

46. Zhao YYS, Ding W. Unilateral versus bilateral pedicle screw fixation in lumbar fusion: a systematic review of overlapping meta-analyses. PLoS ONE. 2019;14(12):e0226848. https://doi.org/10.1371/journal.pone.0226848. Published 2019 Dec 20.

47. Wen JSC, Yu L, Wang S, Xi Y, Ye X. Unilateral versus bilateral percutaneous pedicle screw fixation in oblique lumbar Interbody Fusion. World Neurosurg. 2020;134:e920–7. https://doi.org/10.1016/j.wneu.2019.11.035.

48. Santoni BGHR, McGilvray KC, et al. Cortical bone trajectory for lumbar pedicle screws. Spine J. 2009;9(5):366–73. https://doi.org/10.1016/j.spinee.2008.07.008.

49. Matsukawa KTE, Yato Y, et al. Evaluation of the fixation strength of pedicle screws using cortical bone trajectory: what is the Ideal trajectory for optimal fixation? Spine (Phila Pa 1976). 2015;40(15):E873–8. https://doi.org/10.1097/BRS.0000000000000983.

Publisher's note